



LAWRENCE
LIVERMORE
NATIONAL
LABORATORY

Corrosion-resistant, high-reflectance Mg/SiC multilayer coatings for solar physics in the 25-80 nm wavelength region

R. Soufli, E. T. Al

August 20, 2012

SPIE Space Telescopes and Instrumentation 2012: Ultraviolet
to Gamma Ray
Amsterdam, Netherlands
July 1, 2012 through July 6, 2012

Disclaimer

This document was prepared as an account of work sponsored by an agency of the United States government. Neither the United States government nor Lawrence Livermore National Security, LLC, nor any of their employees makes any warranty, expressed or implied, or assumes any legal liability or responsibility for the accuracy, completeness, or usefulness of any information, apparatus, product, or process disclosed, or represents that its use would not infringe privately owned rights. Reference herein to any specific commercial product, process, or service by trade name, trademark, manufacturer, or otherwise does not necessarily constitute or imply its endorsement, recommendation, or favoring by the United States government or Lawrence Livermore National Security, LLC. The views and opinions of authors expressed herein do not necessarily state or reflect those of the United States government or Lawrence Livermore National Security, LLC, and shall not be used for advertising or product endorsement purposes.

Corrosion-resistant, high-reflectance Mg/SiC multilayer coatings for solar physics in the 25-80 nm wavelength region

Regina Soufli^{1*}, Mónica Fernández-Perea¹, Jeff C. Robinson¹, Sherry L. Baker¹,
Jennifer Alameda¹, Eric M. Gullikson²

¹Lawrence Livermore National Laboratory, Livermore, CA 94550, US

²Lawrence Berkeley National Laboratory, Berkeley, CA 94720, US

ABSTRACT

The corrosion mechanisms in Mg/SiC multilayers have been elucidated and corrosion-resistant Mg/SiC multilayer coatings have been demonstrated using spontaneously intermixed Al-Mg corrosion barrier layers. The corrosion-resistant Mg/SiC multilayers can achieve high reflectance simultaneously in up to three narrow wavelength bands within the 25-80 nm wavelength region, making them attractive candidates for solar physics instrumentation and for other applications.

Keywords: Mg/SiC multilayers, corrosion, EUV reflectance measurements, solar physics.

1. INTRODUCTION

Magnesium/silicon carbide (Mg/SiC)^{1,2,3} is a highly reflective multilayer coating for the 25-80 nm wavelength region with applications including solar and plasma physics, spectroscopy, extreme ultraviolet (EUV) tabletop lasers, high-resolution microscopy, nanopatterning and femtosecond chemistry. Mg/SiC multilayers operate efficiently in the wavelength region from 25 nm (the Mg 2p absorption edge) to 80 nm and beyond. At these wavelengths, Mg absorption remains consistently low and, combined with sharp and stable layer interfaces, produces peak reflectance of 30-50% at near-normal incidence angles. Mg/SiC possesses a unique combination of favorable properties: high reflectance, near-zero film stress, good spectral selectivity and thermal stability up to about 350° C. This combination of superior properties is unmatched by any of the other candidate multilayer material pairs in the > 25 nm wavelength region such as Mo/Si, SiC/Si, Si/B₄C, Al/SiC, Sc/Si and other Mg-based multilayers such as Mg/Co and Mg/Si. However, Mg/SiC multilayers suffer from corrosion, an insidious problem which completely degrades reflectance and has prevented Mg/SiC from being used in applications that require long-term stability, such as mirror coatings for space-borne solar physics telescopes. A few years ago, and based on its unparalleled optical performance, Mg/SiC was initially selected⁴ and applied as the reflective multilayer coating on flight telescope mirrors to image the He II (30.4 nm) and Fe XVI (33.5 nm) solar emission lines for Solar Dynamics Observatory (SDO), NASA's most advanced solar mission currently in orbit. A few months after deposition, corroded areas developed on the Mg/SiC-coated flight mirrors planned for SDO, thus preventing their use. Substitute flight mirrors coated with SiC/Si (instead of Mg/SiC) multilayers were ultimately installed aboard SDO^{5,6,7}, with dramatically decreased the throughput (by a factor of 10) of the 2-mirror imaging telescopes at 30.4 and 33.5 nm, and increased thin film stress across the optical surface of each mirror. More recently, Mg/SiC could have been the most suitable multilayer coating for the Fe XV (28.4 nm) and He II (30.4 nm) channels of the EUV imaging telescopes aboard the Geostationary Operational Environmental Satellite (GOES)-R⁸, the suite of space weather satellites operated by NASA and NOAA. Once again, because of corrosion and based on the experience with the earlier Mg/SiC coatings for the SDO mission, substitute Mo/Si multilayer coatings were applied for the 28.4 nm and 30.4 nm GOES-R channels, with inferior reflectance and stress properties compared to Mg/SiC. Mg/SiC has also been considered as mirror coating for future EUV solar missions, but its implementation continues to be hindered by the corrosion issue⁹.

We recently elucidated for the first time the origins and mechanisms of corrosion propagation in Mg/SiC multilayers. Following these findings, we demonstrated efficient corrosion barrier structures for Mg/SiC multilayers^{10,11}. The barriers

* e-mail: regina.soufli@llnl.gov, phone: 925-422-6013.

consist of nanometer-scale Al and Mg layers that intermix spontaneously to produce a partially amorphous Al-Mg layer. The barriers are inserted in key locations within the Mg/SiC multilayer coating and are shown to prevent atmospheric corrosion while maintaining the unique combination of favorable Mg/SiC reflective properties. Furthermore, we have developed and experimentally demonstrated corrosion-resistant Mg/SiC multilayer concepts with high reflectance at up to three narrowband multilayer interference orders, thus offering the possibility for single, double, or triple-wavelength operation¹². The concept of imaging multiple wavelengths using a single multilayer coating^{13,14} could significantly ease the cost, risk and complexity of future solar missions. For example, an existing practice towards the imaging of multiple wavelengths from a single telescope is to divide each telescope mirror in multiple sectors, with each sector tuned to one specific wavelength and coated separately using the appropriate material pair. This approach requires the development of several different multilayer coatings and the use of a hardware mask placed on top of the mirror during multilayer deposition, which involves additional complexities and risks^{4,5,6,7,8}. The instrument throughput corresponding to each wavelength is also decreased accordingly. Moreover, multiple telescopes often have to be employed in a given mission^{4,5,6,7} in order to achieve the number of EUV channels required to accomplish the science objectives. This comes at the expense of increased payload mass. The development of Mg/SiC multilayer coatings with high reflectance in multiple narrow wavelength bands in the 25-80 nm wavelength region has the potential to mitigate all aforementioned issues.

2. EXPERIMENTAL FACILITIES

Mg/SiC films were deposited in a planar DC-magnetron sputtering deposition system¹⁵ located at Lawrence Livermore National Laboratory (LLNL). The base vacuum pressure in the deposition chamber was around 10^{-8} Torr and argon (Ar) was used as process gas at 10^{-3} Torr. Temperature was maintained below 70° C during deposition. The quoted sputtering source (target) purity was 99.97 wt. % for Mg, 99.9999 wt. % for SiC and 99.9995 wt. % for Al. The surface dimensions of each sputtering target were $559 \times 127 \text{ mm}^2$. Sputtering targets were operated at 1200 W (Mg), 2000 W (SiC, Figs. 1 and 2), 1000 W (SiC, Fig. 3) and 2000 W (Al). After deposition, all samples were stored and handled under identical conditions, in ambient laboratory environment. The Scanning Electron Microscopy (SEM) images in Figs. 1(a), 1(c) and 2(a) were obtained with a Leo 1560TM instrument at LLNL, operated at 3 kV voltage and equipped with a Gemini[®] field emission column and an in-lens annular detector. The image in Fig. 1(b) was obtained at EAG Labs with a JEOL 2010 Transmission Electron Microscopy (TEM) instrument equipped with a 1 Mpixel camera. The image in Fig. 2(b) was obtained at EAG Labs with an FEI TecnaiTM TEM instrument equipped with a 4 Mpixel camera. The thickness (in the direction perpendicular to the image plane) of the cross-section specimens shown in the TEM images in Figs. 1(b) and 2(b) was estimated at 100 nm. The EUV reflectance measurements shown in Fig. 3 were performed at beamline 6.3.2. of the Advanced Light Source (ALS) synchrotron at Lawrence Berkeley National Laboratory. The general characteristics of the beamline have been described in detail earlier^{16,17}. Two gratings (80 and 200 lines/mm) were used in the monochromator to access the wavelength range 11-50 nm. The monochromator exit slit was set to a width of 40 μm . Wavelength calibration was based on the 2p absorption edges of Al and Si transmission filters with a relative accuracy of 0.011% rms, and could be determined with 0.007% repeatability. During the measurements, 2nd harmonic and stray light suppression was achieved with a series of transmission filters (Mg, Al, Si, Be). For higher-order harmonic suppression, an “order suppressor” consisting of three carbon-coated mirrors at a variable grazing incidence angle (depending on wavelength range) and based on the principle of total external reflection was used in addition to the filters. The ALS storage ring current was used to normalize the signal against the storage ring current decay. The signal was collected on a GaAsP photodiode detector, with 1 degree angular acceptance. Reflectance was measured with $\pm 1\%$ relative accuracy, dominated by the GaAsP photodiode uniformity in each wavelength range. The vacuum pressure in the measurement chamber was in the range 2×10^{-6} - 10^{-7} Torr.

3. EXPERIMENTAL RESULTS AND DISCUSSION

Atmospheric corrosion in Mg/SiC multilayers appears as spots, which sporadically appear on the top surface and grow over time. Fig. 1(a) shows detailed topography from a standard Mg/SiC multilayer aged for 3 years after deposition, with advanced corrosion visible to the eye. The as-designed multilayer structure of the depicted sample consists of a 100-mm diameter, 500- μm thickness Si (100) wafer substrate, coated with a film of total thickness $d_{\text{total}} = \{ (d_{\text{SiC, base}} + [20 \times (d_{\text{SiC}} + d_{\text{Mg}})] + d_{\text{SiC, top}}) \} = 512 \text{ nm}$, where $d_{\text{SiC, base}} = 3 \text{ nm}$ is the thickness of a bottom SiC layer, followed by a periodic multilayer structure consisting of $N=20$ Mg/SiC bilayers (periods) with period thickness $d_{\text{SiC}} + d_{\text{Mg}} = 6 \text{ nm} + 19 \text{ nm} = 25 \text{ nm}$, followed by a top SiC capping layer with thickness $d_{\text{SiC, top}} = 9 \text{ nm}$. The multilayer was designed to have its peak

reflectance at wavelength $\lambda = 46.3$ nm at $\theta = 85$ degrees (near-normal) incidence angle. Several areas in Fig. 1(a) appear to have undergone a process of volume expansion, have erupted and are peeling off the top while still being partially attached to the top surface, thus exposing the inner layers in the multilayer. In other areas, material has been entirely removed from the top of the multilayer and is missing. Fig. 1(b) shows a cross-sectional TEM image of the multilayer, obtained on one of the erupted areas where the inner layers are exposed. It was determined in Ref. 11 that the regions with “cellular” appearance are Mg corrosion products, a mixture of $\text{Mg}(\text{OH})_2$, $\text{Mg}(\text{CO})_3$ and MgO . Formation of these Mg corrosion products is accompanied by volume expansion and leads to the eruptive effects seen in Fig. 1(a). In Fig. 1(b), 4 Mg/SiC bilayers (out of a total of $N=20$ Mg/SiC bilayers deposited initially) have been consumed by corrosion and are missing from the top of the multilayer film. As is explained in Ref. 11, and provided that the substrate surface is sufficiently clean, corrosion attacks the multilayer film from the top surface at local entry points such as pinholes, particles and grain boundaries inherent in sputtered thin films. Such defects provide pathways for humidity and reactive ions (O^{2-} , OH^- , Cl^-) present in the environment to reach the topmost Mg layers. Fig. 1(c) shows early, pre-eruptive stages of corrosion from a Mg/SiC multilayer with the same design parameters as described above. Additional TEM analysis, discussed in Ref. 11, showed that on the sample of Fig. 1(c) thin layers of Mg corrosion products have formed just underneath the SiC capping layer. The corroded areas appear as bright spots in the top-view SEM image of Fig. 1(c), but are not visible to the eye.

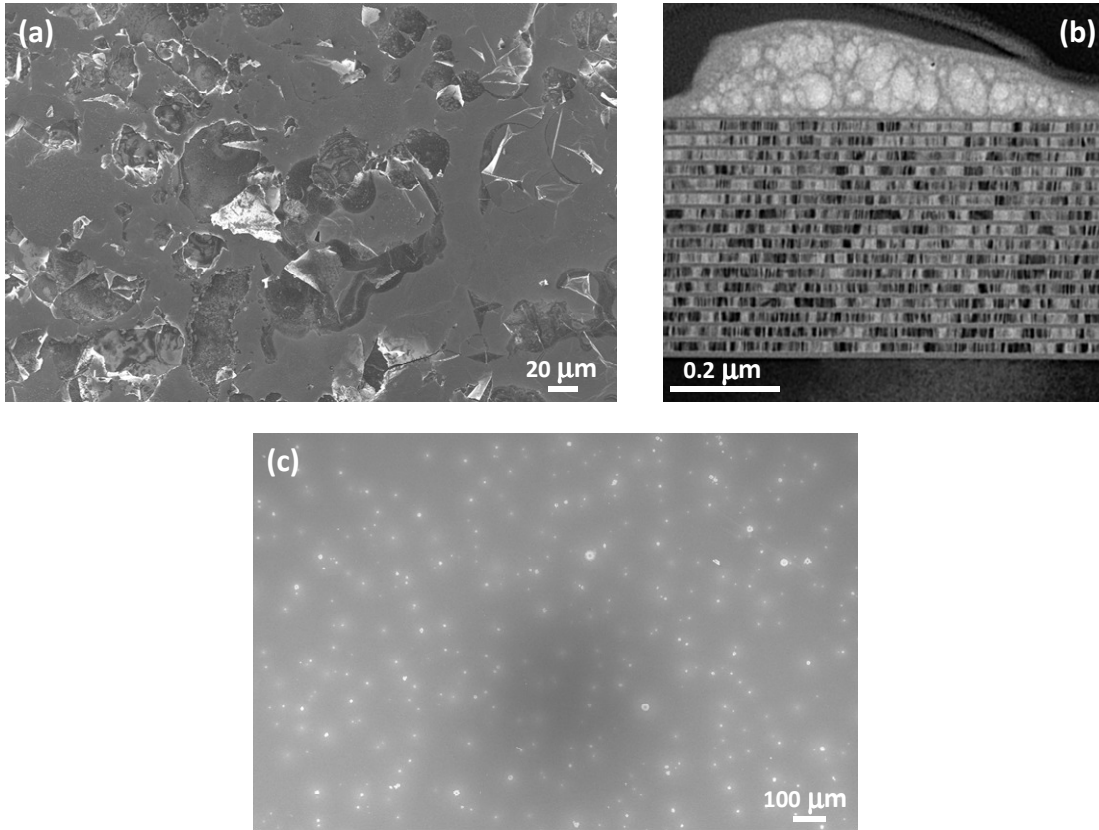


Fig. 1: (a) SEM image of the top surface of severely corroded Mg/SiC multilayer film aged for 3 years. Several regions appear to have material partially or entirely delaminated from the top surface, with inner layers of the multilayer being exposed. (b) Cross-sectional TEM image of Mg/SiC multilayer obtained from one of the severely corroded regions shown in Fig. 1(a). A formation with “cellular” appearance (consisting of Mg corrosion products) is shown on top of 16 un-disturbed Mg/SiC bilayers. 4 Mg/SiC bilayers are missing from the top of the multilayer stack - they have been consumed by corrosion. (c) SEM image of the top surface of a Mg/SiC multilayer film with initial stages of corrosion, aged for 3 years. The areas appearing as bright spots are corroded regions, with a thin layer of Mg corrosion products having formed just underneath the SiC capping layer.

The Mg/SiC corrosion barrier structures we developed recently, reduce corrosion dramatically while maintaining all the favorable reflective properties of Mg/SiC multilayers. A corrosion-resistant Mg/SiC multilayer, aged for 3 years after deposition, is shown in Figure 2. A comparison of Fig. 2(a) with Figs. 1(a) and 1(c) demonstrates the dramatic reduction of corrosion in the new, corrosion-resistant multilayers. The multilayer in Fig. 2 consists of the same structure as the multilayer in Fig. 1, with the addition of: (i) a 20 nm-thick Al layer above the topmost Mg layer and (ii) another 20 nm-thick Al layer inserted at the bottom of the multilayer, on top of the Si substrate. The top Al layer intermixes spontaneously with the top Mg layer to form a partially amorphous Al-Mg layer, shown in Fig. 2(b), which acts as the primary corrosion barrier. The Al-Mg corrosion barrier layer was inserted underneath the SiC capping layer for protection from exposure to air. The corrosion barrier can be inserted in multiple locations (including at the bottom) of the multilayer stack, with minimal or no impact in peak reflectivity. The relative transparency of Al in the 25-80 nm wavelength range is extremely beneficial towards maintaining high reflectance. A more detailed analysis of the physical properties of the Al-Mg corrosion barrier layer can be found in Ref. 11.

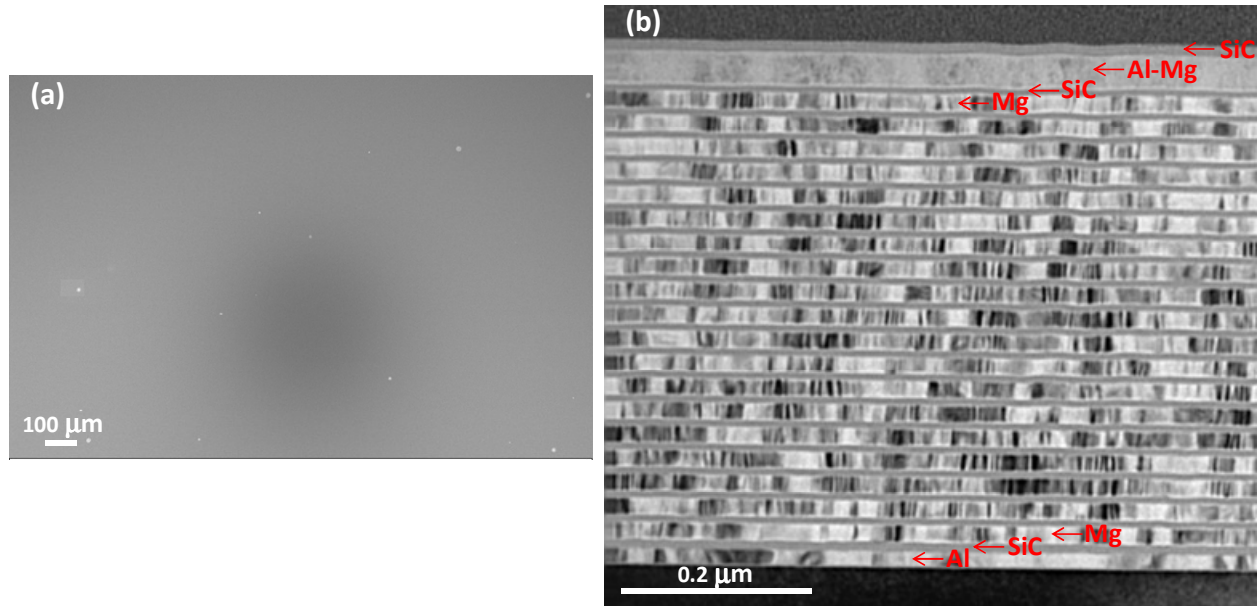


Fig. 2: Images from a corrosion-resistant Mg/SiC multilayer film aged for 3 years. (a) SEM image of top surface. A comparison with Figs. 1(a) and 1(c) demonstrates the dramatic reduction of corrosion in the corrosion-resistant Mg/SiC. (b) Cross-sectional TEM image of multilayer. The partially amorphous Al-Mg corrosion barrier is shown, as well as the polycrystalline Mg layers, the amorphous SiC layers and the polycrystalline Al layer at the bottom of the multilayer stack.

The ability of corrosion-resistant Mg/SiC multilayers to achieve high reflectance simultaneously for multiple narrowband peaks (multilayer interference orders) in an extended wavelength range is demonstrated in Fig. 3 and is discussed in more detail in Ref. 12. The as-designed multilayer structure of the sample in Fig. 3 utilizes the same corrosion barrier concept as shown in Fig. 2(b), but with $N=10$ Mg/SiC bilayers and with differently optimized Al, Mg and SiC thicknesses in order to achieve the reflective performance shown in Fig. 3. Measurements in the wavelength region longer than 50 nm (not shown in Fig. 3) were also obtained and discussed in Ref. 12, and the measured results are in good agreement with the model predictions. The multilayer shown in Fig. 3 has consistently high reflectance for the first 3 interference order peaks and remarkably high reflectance for the 1st order peak at 78.1 nm, in a wavelength region with extremely limited availability of other efficient multilayer material systems¹². It should be noted that the 25-80 nm wavelength region contains a wealth of plasma emission lines of interest for solar physics and many other disciplines: Fe XV (28.4 nm), He II (30.4 nm), Fe XVI (33.5 nm), Ne VII (46.5 nm) and O IV / Ne VIII (78 nm), to name just a few. The design of corrosion-resistant Mg/SiC multilayer coatings could therefore be customized (with periodic, aperiodic or “stacked” concepts), so that the multilayer peak wavelengths coincide with the emission lines of interest for the application. The development of efficient corrosion barrier layers combined with innovative multilayer designs will enable Mg/SiC multilayer coatings to reach their full potential.

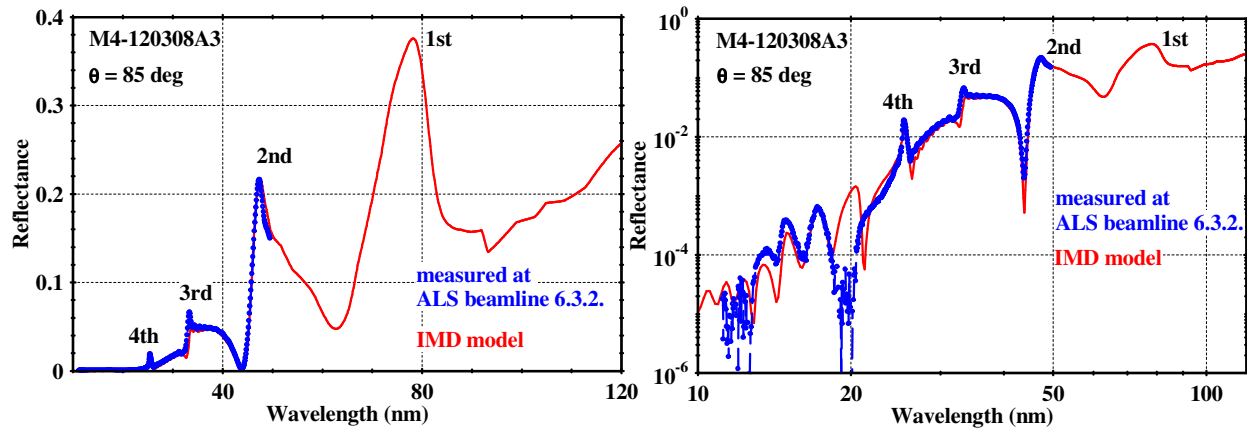


Fig. 3: Measured and modeled reflectance of corrosion-resistant, triple-wavelength Mg/SiC multilayer. To model the measured reflectance, the IMD software¹⁸ was used with a compilation of experimental optical constants^{19,20,21}. **Left:** Reflectance is plotted on linear axes over an extended wavelength range. The 1st through 4th multilayer interference orders are shown. **Right:** Reflectance is plotted on logarithmic axes, showing fine structure and higher multilayer interference orders.

ACKNOWLEDGEMENTS

This work was performed under the auspices of the U.S. Department of Energy by Lawrence Livermore National Laboratory under Contract DE-AC52-07NA27344 and by the University of California Lawrence Berkeley National Laboratory under Contract No. DE-AC03-76F00098. The Advanced Light Source is supported by the Director, Office of Science, Office of Basic Energy Sciences, of the U.S. Department of Energy under Contract No. DE-AC02-05CH11231. Funding was provided in part by LLNL's Laboratory Directed Research and Development Program. The contributions of Harry Kawayoshi, Jiafang Lu and Martin Izquierdo (Evans Analytical Labs, Sunnyvale, California) in the acquisition of the TEM images is gratefully acknowledged.

REFERENCES

- ¹ H. Takenaka, S. Ichimaru, T. Ohchi, and E. M. Gullikson, J. Electron Spectrosc. Relat. Phenom. **144-147**, 1047-1049 (2005).
- ² A. Aquila, F. Salmasi, Y. Liu, and E. M. Gullikson, Optics Express **17**, 22102-22107 (2009).
- ³ D. S. Martínez-Galarce, P. Boerner, R. Soufli, B. De Pontieu, N. Katz, A. Title, E. M. Gullikson, J. C. Robinson, S. L. Baker Proc. SPIE **7011**, 70113K (2008).
- ⁴ R. Soufli, D. L. Windt, J. C. Robinson, S. L. Baker, E. A. Spiller, F. J. Dollar, A. L. Aquila, E. M. Gullikson, B. Kjornrattanawanich, J. F. Seely, and L. Golub, Proc. SPIE **5901**, 59010M (2005).
- ⁵ J. R. Lemen, *et al*, Solar Physics **275**, 41-66 (2012).
- ⁶ P. Boerner, *et al*, Solar Physics **275**, 17-40 (2012).
- ⁷ R. Soufli, E. Spiller, D. L. Windt, J. C. Robinson, E. M. Gullikson, L. Rodríguez-de Marcos, Mónica Fernández-Perea, S. L. Baker, A. L. Aquila, F. J. Dollar, J. Antonio Méndez, Juan I. Larruquert, L. Golub, P. Boerner, SPIE Proc. **8443** (2012), this Conference Proceedings.
- ⁸ D. Martínez-Galarce, R. Soufli, D. L. Windt, M. Bruner, E. Gullikson, S. Khatri, E. Spiller, J. Robinson, S. Baker and E. Prast, SPIE Proc. **8501** (2012).
- ⁹ M.G. Pelizzo, A. J. Corso, P. Zuppella, P. Nicolosi, S. Fineschi, J. Seely, B. Kjornrattanawanich, and D. L. Windt, Opt. Eng. **51**, 023801 (2012).
- ¹⁰ R. Soufli, M. Fernández-Perea, J. C. Robinson, S. L. Baker, "Corrosion-resistant multilayer coatings for the 25-75 nm wavelength region", 2011 International Workshop on EUV and Soft X-ray Sources, University College Dublin, Ireland, November 7-9, 2011. <http://www.euvlitho.com/2011/S17.pdf>
- ¹¹ R. Soufli, M. Fernández-Perea, S. L. Baker, J. C. Robinson, J. Alameda, and C. C. Walton, Appl. Phys. Lett. **101**, 043111 (2012).
- ¹² M. Fernández-Perea, R. Soufli, J. C. Robinson, L. Rodríguez-de Marcos, J. A. Mendez, J. I. Larruquert and E. M. Gullikson, submitted to Optics Express (2012).
- ¹³ C. Hecquet, F. Delmotte, M.-F. Ravet-Krill, S. de Rossi, A. Jérôme, F. Bridou, F. Varnière, E. Meltchakov, F. Auchère, A. Giglia, N. Mahne, and S. Nannarone, Appl. Phys. A **95**, 401-408 (2009).
- ¹⁴ T. Ejima, Y. Kondo, M. Watanabe, Jpn. J. Appl. Phys. **40**, 376-379 (2001).

-
- ¹⁵ R. Soufli, R. M. Hudyma, E. Spiller, E. M. Gullikson, M. A. Schmidt, J. C. Robinson, S. L. Baker, C. C. Walton, and J. S. Taylor, Appl. Opt. **46**, 3736-3746 (2007).
- ¹⁶ J. H. Underwood and E. M. Gullikson, J. Electr. Spectr. Rel. Phenom. **92**, 265-272 (1998).
- ¹⁷ E. M. Gullikson, S. Mrowka, B. B. Kaufmann, Proc. SPIE **4343**, 363-373 (2001).
- ¹⁸ D. L. Windt, Computers in Physics **12**, 360-370 (1998).
- ¹⁹ M. Vidal-Dasilva, A. L. Aquila, E. M. Gullikson, F. Salmassi, and J. I. Larruquert, J. Appl. Phys. **108**, 063517 (2010).
- ²⁰ J. B. Kortright and D. L. Windt, Appl. Opt. **27**, 2841-2846 (1988).
- ²¹ E. Shiles, T. Sasaki, M. Inokuti, and D. Y. Smith, Phys. Rev. B **22**, 1612-1628 (1980).